

Electrical impedance tomography and Mittag-Leffler's function

M Ikehata¹ and S Siltanen^{1,2}

¹ Department of Mathematics, Faculty of Engineering, Gunma University, Kiryu 376-8515, Japan

² Instrumentarium Imaging (GE Medical Systems), Finland

Abstract.

Given a two-dimensional bounded domain and a conductivity distribution, how to extract information about unknown inclusions in conductivity from finitely many noisy Cauchy data? (In practice, the data are given by electrical impedance tomography (EIT) measurements.) First, a direct approach is presented, based on an extraction formula of the set of all points in the domain that can be connected with infinity by a straight line without intersecting the closure of the inclusions. The formula uses an indicator function that depends on a large parameter τ and can be calculated from infinitely many non-noisy Cauchy data. Second, a modified indicator function is defined. It can be calculated from finitely many noisy Cauchy data. Its properties are studied; the results suggest how much data is needed and how to choose τ . Third, a regularized algorithm that is based on the theoretical study is given for extracting inclusions approximately. Choice of all parameters is described explicitly. Numerical examples using simulated continuum data show that a reliable estimate for the number and location of inclusions is achieved. However, the shape of the inclusions is not recovered.

Revision 1 of the submitted version 17 (figures 6 and 8 modified), April 20, 2004

1. Introduction

Let Ω be a bounded domain in \mathbb{R}^2 with C^2 boundary. We consider an inverse problem for the equation

$$\nabla \cdot \gamma \nabla u = 0 \quad \text{in } \Omega. \quad (1.1)$$

Here γ is a $L^\infty(\Omega)$ coefficient satisfying $\gamma(x) \geq C$ for almost all $x \in \Omega$ and for some constant $C > 0$. Given $f \in H^{1/2}(\partial\Omega)$ there exists a unique weak solution $u \in H^1(\Omega)$ of equation (1.1) satisfying $u = f$ on $\partial\Omega$.

The map

$$\Lambda_\gamma : f \longmapsto \gamma \frac{\partial u}{\partial \nu} \Big|_{\partial\Omega}$$

is called the Dirichlet-to-Neumann map. Here ν denotes the unit outward normal relative to $\partial\Omega$. Physically γ denotes the conductivity of Ω , f the voltage potential applied on $\partial\Omega$ and $\Lambda_\gamma f$ the resulting electric current density on $\partial\Omega$. Calderón's problem, formulated in [7], is to extract information about general γ from Λ_γ . This problem is a mathematical model for electrical impedance tomography (EIT). The aim of EIT is to produce images of electric conductivity distribution inside given body from the knowledge of boundary currents and voltages. It has applications in medical imaging, geophysics, industrial process monitoring and nondestructive evaluation (see

[2, 3, 9] for reviews). However, we will not consider this general problem and refer the reader to [28, 29, 32, 33, 4, 25, 27, 31, 24].

In this paper, we assume that γ takes the form

$$\gamma(x) = \begin{cases} 1, & \text{if } x \in \Omega \setminus D, \\ 1 + h(x), & \text{if } x \in D. \end{cases}$$

Here D is an open subset of Ω with Lipschitz boundary, satisfies $\overline{D} \subset \Omega$ and $h(\neq 0)$ is an essentially bounded function on D . The pair (D, h) is a mathematical model of inclusions or defects in the material Ω with a constant conductivity 1. Note that we do not assume that D has special geometry.

The problem is to extract information about D from noisy data $f + \mathcal{E}_1$ and $\Lambda_\gamma f + \mathcal{E}_2$ for known finitely many f when D and h are unknown and $\mathcal{E}_1, \mathcal{E}_2 \in L^2(\partial\Omega)$. These data are given by the continuum model for EIT.

The spirit of the approach presented in this paper is already described in [18]. First we seek an *extraction formula* for extracting information about D from non-noisy data. Next we consider how to modify the extraction formula for the case of noisy data and prove the convergence of the modified formula, called *regularized extraction formula*, when noise level tends to zero. In [16], the first author established an extraction formula of the support function of D . The formula uses $\Lambda_\gamma f$ for a single given nonconstant f , however, D is assumed to be polygonal and h constant. In [18] the corresponding regularized extraction formula is given. See [19] for a numerical implementation.

In this paper, we employ this approach in spirit; however, the extraction formula which is the base of the approach is taken from [17]. Therein the first author considered extracting information about the location of D from an infinite number of non-noisy Cauchy data, i.e. $\Lambda_\gamma f$ for known infinitely many f . Here we present the result in a simpler form, but the proof can be done along the same lines.

Definition 1.1 We say that a point in Ω is visible if it can be connected with infinity by a straight line without intersecting \overline{D} . We denote by $V(D)$ the set of all points in Ω that are visible. It is trivial to see that $\overline{D} \subset \Omega \setminus V(D)$.

In [17] the first author gave an extraction formula of $V(D)$ from Λ_γ . More precisely, given $\alpha \in]0, 1[$ let $E_\alpha(z)$ denote Mittag-Leffler's function

$$E_\alpha(z) = \sum_{m=0}^{\infty} \frac{z^m}{\Gamma(\alpha m + 1)}.$$

This is an entire function whose modulus grows exponentially in the cone of opening angle $\alpha\pi/2$ about the positive real axis and decays algebraically outside the cone as $z \rightarrow \infty$, see [1]. See Figure 1 for a plot of $|E_{1/2}(z)|$.

Denote $S^1 = \{x \in \mathbb{R}^2 : |x| = 1\}$. Given $\omega = (\omega_1, \omega_2) \in S^1$ set $\omega^\perp = (-\omega_2, \omega_1)$. For any $y \in \mathbb{R}^2$ define a harmonic function depending on $\tau > 0$ by the equation

$$e_\tau^\alpha(x; y, \omega) = E_\alpha(\tau\{(x - y) \cdot \omega + i(x - y) \cdot \omega^\perp\}), \quad x \in \mathbb{R}^2. \quad (1.2)$$

Definition 1.2 Define the indicator function by the formula

$$I_{(y, \omega)}^\alpha(\tau) = \int_{\partial\Omega} \{(\Lambda_\gamma - \Lambda_1)e_\tau^\alpha(\cdot; y, \omega)|_{\partial\Omega}\} \overline{e_\tau^\alpha(\cdot; y, \omega)|_{\partial\Omega}} d\sigma.$$

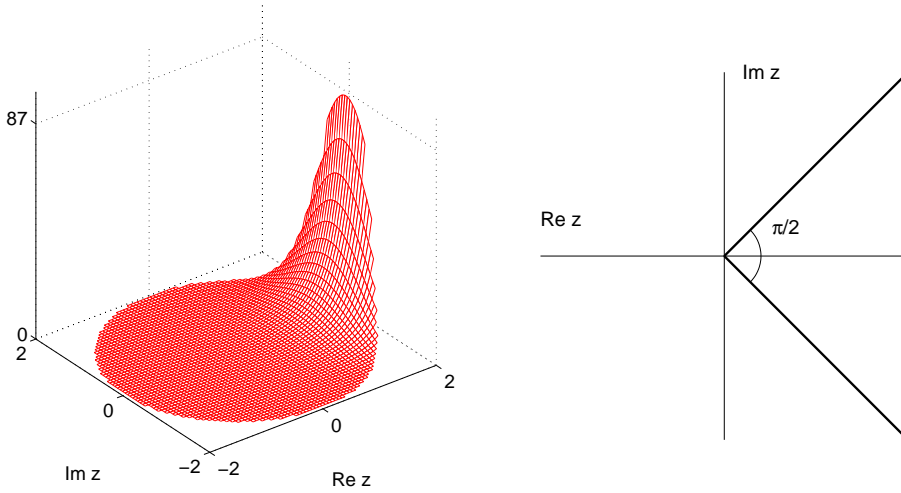


Figure 1. Left: plot of the absolute value of Mittag-Leffler's function $E_{1/2}(z)$ in the disc $|z| \leq 2$. Right: the function $|E_{1/2}(z)|$ grows exponentially when $z \rightarrow \infty$ inside this cone. Outside the cone, the function decays algebraically.

Let $C_y(\omega, \pi\alpha/2)$ denote the interior of the cone about ω of opening angle $\pi\alpha/2$ with vertex at y (see Figure 2):

$$C_y(\omega, \pi\alpha/2) = \{x \in \mathbb{R}^2 \mid (x - y) \cdot \omega > |x - y| \cos(\pi\alpha/2)\}.$$

It is easy to see that the point y in Ω is visible if and only if there exist $\alpha \in]0, 1[$ and $\omega \in S^1$ such that $\overline{\{C_y(\omega, \pi\alpha/2)\}} \cap \overline{D} = \emptyset$.

Theorem 1.1 characterizes $V(D)$ in terms of $\Lambda_\gamma f$ for known infinitely many f .

Theorem 1.1 ([17]) *Assume that there exists a positive constant C such that $h(x) \geq C$ (or $-h(x) \geq C$) for almost all $x \in D$. Given $(y, \omega) \in \Omega \times S^1$ we have:*

if $\overline{\{C_y(\omega, \pi\alpha/2)\}} \cap \overline{D} = \emptyset$, then

$$\lim_{\tau \rightarrow \infty} |I_{(y, \omega)}^\alpha(\tau)| = 0;$$

if $\overline{\{C_y(\omega, \pi\alpha/2)\}} \cap \overline{D} \neq \emptyset$ and $C_y(\omega, \pi\alpha/2) \cap D = \emptyset$, then

$$\liminf_{\tau \rightarrow \infty} |I_{(y, \omega)}^\alpha(\tau)| > 0;$$

if $C_y(\omega, \pi\alpha/2) \cap D \neq \emptyset$, then

$$\lim_{\tau \rightarrow \infty} |I_{(y, \omega)}^\alpha(\tau)| = \infty.$$

See Figure 3. Theorem 1.1 is a generalization of a result of [14] in which the first author introduced the enclosure method. The enclosure method was realized numerically in [20] and, independently, in [5]. The method is based on the asymptotic behavior of the harmonic function $\exp(\tau(x \cdot \omega + ix \cdot \omega^\perp))$ as $\tau \rightarrow \infty$ instead of (1.2). Note that $E_\alpha(z) \rightarrow e^z$ as $\alpha \rightarrow 1$. See [15] for other applications of the enclosure method.

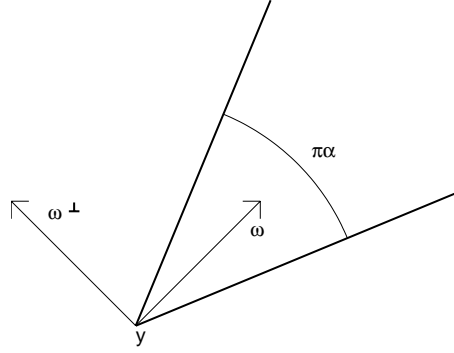


Figure 2. The cone $C_y(\omega, \pi\alpha/2)$. Note that the *opening angle* $\pi\alpha/2$ of the cone is half of the angle $\pi\alpha$ between its sides.

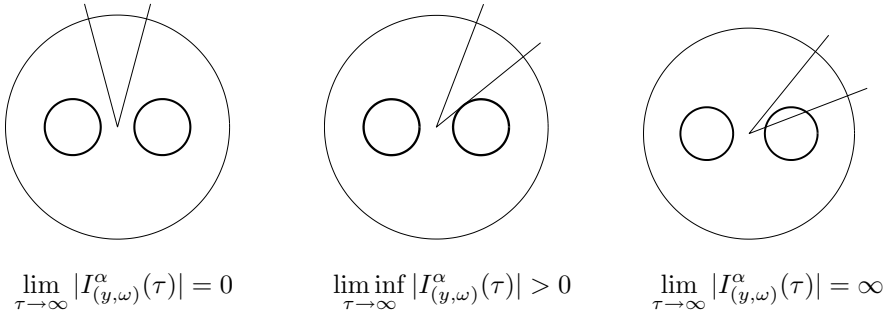


Figure 3. According to Theorem 1.1, knowledge of the indicator function can be used to determine whether or not a given cone intersects the inclusion D . Here Ω is the unit disc and D is the union of two open discs. See [17] for proof.

From theorem 1.1 we obtain the extraction formula of $V(D)$:

$$V(D) = \bigcup_{0 < \alpha < 1} \bigcup_{\omega \in S^1} \{y \in \Omega \mid \lim_{\tau \rightarrow \infty} |I_{(y,\omega)}^\alpha(\tau)| = 0\}. \quad (1.3)$$

Formula (1.3) is based on the assumption that one can know the data $e_\tau^\alpha(\cdot; y, \omega)|_{\partial\Omega}$ and $(\Lambda_\gamma - \Lambda_1)(e_\tau^\alpha(\cdot; y, \omega)|_{\partial\Omega})$ exactly. However, this is impossible in practical EIT. We regularize formula (1.3) so that it works in the case of finitely many noisy data.

In practice we have two limitations: the finite number of electrodes attached on the surface of the body and the finite accuracy of the data. This implies that one cannot take τ large. We suggest an algorithm for obtaining information about the location of D when τ is small (we give an explicit choice of τ depending on the number of electrodes and of the domain Ω). The algorithm is based on finding cones $C_y(\omega, \pi/4)$ for which the indicator function has a minimum with respect to the angular variable ω , and assuming that a narrow cone $C_y(\omega, \pi/32)$ does not intersect D .

Numerical detection of inclusions in conductivity has been discussed by several authors. The probe method was introduced in [12] (see also [13] for further investigation of the probe method). The enclosure method was implemented in [20, 5]. An application of the factorization method introduced in [23] to the present problem

is given in [5]. See [10, 21] for level set methods and [22, 26] for statistical inversion. Methods for small inhomogeneities were given in [6, 8]. The point source method was used in [11] for the reconstruction of a perfectly conducting inclusion from one boundary measurement.

A brief outline of this paper is as follows. The main result is described in Section 2 and proved in Section 5. The proof is based on the relationship between three indicator functions as defined in Sections 1, 2 and 4. To study their relationship we require some properties of Mittag-Leffler's function; these are found in Section 3. In Section 6 we mention the corresponding results in the case when the Dirichlet-to-Neumann map is replaced with the Neumann-to-Dirichlet map. In Section 7 we describe our algorithm for obtaining information about the location of D . In Section 8 we give numerical results with simulated noisy continuum data. We conclude our results in Section 9.

Remark 1.1 Throughout the paper always assume that: there exists a positive constant C such that $h(x) \geq C$ for almost all $x \in D$ or $-h(x) \geq C$ for almost all $x \in D$. However, D , h and C are unknown.

2. Main result

In this section we modify Theorem 1.1 to cover the case of finitely many noisy measurements. Our main results, Theorem 2.1 and Corollary 2.1, show that the situation depicted in Figure 3 holds asymptotically when the number of measurements grows and noise level tends to zero.

Let $n \geq 2$ and $N \geq 1$. Given $\delta > 0$ let $\mathcal{E}^{j,nN} = (\mathcal{E}_0^j, \dots, \mathcal{E}_{nN}^j) \in \{L^2(\partial\Omega)\}^{nN+1}$, $j = 1, 2$ satisfy

$$\|\mathcal{E}\| = \|(\mathcal{E}^{1,nN}, \mathcal{E}^{2,nN})\| \equiv \max_{j=1,2} \max_{0 \leq m \leq nN} \|\mathcal{E}_m^j\|_{L^2(\partial\Omega)} \leq \delta. \quad (2.1)$$

Here δ denotes the upper bound of the size of noise.

Definition 2.1 Let $(y, \omega) \in \Omega \times S^1$. Define the noisy truncated indicator function by the formula

$$\begin{aligned} I_{(y, \omega)}^{1/n, nN}(\tau; \mathcal{E}) &= \sum_{0 \leq m, l \leq nN} \frac{\tau^{m+l}}{\Gamma(\frac{m}{n} + 1)\Gamma(\frac{l}{n} + 1)} \\ &\quad \times \int_{\partial\Omega} \{(\Lambda_\gamma - \Lambda_1)(\{(x-y) \cdot (\omega + i\omega^\perp)\}^m |_{\partial\Omega}) + \mathcal{E}_m^1(x)\} \\ &\quad \cdot \overline{\{(x-y) \cdot (\omega + i\omega^\perp)\}^l + \mathcal{E}_l^2(x)} d\sigma(x). \end{aligned}$$

This function can be calculated from noisy current densities

$$(\Lambda_\gamma - \Lambda_1)(\{(x-y) \cdot (\omega + i\omega^\perp)\}^m |_{\partial\Omega}) + \mathcal{E}_m^1(x), \quad m = 0, \dots, nN,$$

and noisy voltages

$$\{(x-y) \cdot (\omega + i\omega^\perp)\}^l + \mathcal{E}_l^2(x), \quad l = 0, \dots, nN.$$

We consider how to extract an approximation of $V(D)$ from $I_{(y, \omega)}^{1/n, nN}(\tau; \mathcal{E})$ when δ is known and small. Before stating the theorem we need some definitions.

Let $c_y (> 0)$ satisfy

$$c_y \geq \sup_{x \in \Omega} |x - y|. \quad (2.2)$$

Let β_0 denote the unique positive solution of the equation

$$\frac{2}{e}\beta + \log \beta = 0. \quad (2.3)$$

β_0 satisfies $1/\sqrt{e} < \beta_0 < 1$. We assume that, given $\beta \in]0, \beta_0[$ and $\theta \in]0, 1[$, the noise level δ satisfies

$$0 < \delta \leq \exp\left\{-\frac{\beta}{\theta e} \frac{c_y^n + 1}{c_y^n}\right\}. \quad (2.4)$$

Given real number c we denote by $[c]$ the largest integer that does not exceed c . Define

$$N_\theta^\beta(\delta; y) = \left[-\frac{\theta e c_y^n \log \delta}{\beta c_y^n + 1}\right] \quad (2.5)$$

and

$$\tau_y^{1/n, \beta}(N) = \left(\frac{N + \frac{1}{n}}{e}\right)^{1/n} \frac{\beta^{1/n}}{c_y}. \quad (2.6)$$

We are ready to give our main result. Compare it to Theorem 1.1 and Figure 3.

Theorem 2.1 *Let $n \geq 2$ and $\alpha = 1/n$. For $N = N_\theta^\beta(\delta; y)$ we have:*

if $\overline{\{C_y(\omega, \pi\alpha/2)\}} \cap \overline{D} = \emptyset$, then

$$\lim_{\delta \rightarrow 0} \left(\sup_{\|\mathcal{E}\| \leq \delta} |I_{(y, \omega)}^{1/n, nN}(\tau_y^{1/n, \beta}(N); \mathcal{E})| \right) = 0;$$

if $\overline{\{C_y(\omega, \pi\alpha/2)\}} \cap \overline{D} \neq \emptyset$ and $C_y(\omega, \pi\alpha/2) \cap D = \emptyset$, then

$$\liminf_{\delta \rightarrow 0} \left(\inf_{\|\mathcal{E}\| \leq \delta} |I_{(y, \omega)}^{1/n, nN}(\tau_y^{1/n, \beta}(N); \mathcal{E})| \right) > 0;$$

if $C_y(\omega, \pi\alpha/2) \cap D \neq \emptyset$, then

$$\lim_{\delta \rightarrow 0} \left(\inf_{\|\mathcal{E}\| \leq \delta} |I_{(y, \omega)}^{1/n, nN}(\tau_y^{1/n, \beta}(N); \mathcal{E})| \right) = \infty.$$

Theorem 2.1 is a direct consequence of Theorem 4.1 and Proposition 5.1 described in Sections 4 and 5, respectively. Note that $\tau_y^{1/n, \beta}(N_\theta^\beta(\delta; y)) \rightarrow \infty$ as $\delta \rightarrow 0$ and the order of blowing up is $|\log \delta|^{1/n}$.

Remark 2.1 Given $\theta \in]0, 1[$ set $\beta = \beta_0 \theta \in]0, \beta_0[$. Then (2.4) and (2.5) become

$$0 < \delta \leq \exp\left\{-\frac{\beta_0}{e} \frac{c_y^n + 1}{c_y^n}\right\} \quad \text{and} \quad N_\theta^\beta(\delta; y) = \left[-\frac{e c_y^n \log \delta}{\beta_0 c_y^n + 1}\right],$$

respectively. These are independent of θ . However, (2.6) becomes

$$\tau_y^{1/n, \beta}(N) = \left(N + \frac{1}{n}\right)^{1/n} \left(\frac{\beta_0}{e}\right)^{1/n} \frac{\theta^{1/n}}{c_y}$$

and depends on θ . Under these choices, Theorem 2.1 is still valid.

For calculating $I_{(y, \omega)}^{1/n, nN}(\tau; \mathcal{E})$ we need still infinitely many noisy Cauchy data. Next we reduce it to finitely many data. The point is the formula

$$\{(x - y) \cdot (\omega + i\omega^\perp)\}^m = \sum_{r=0}^m (\omega_1 - i\omega_2)^m \binom{m}{r} (-1)^{m-r} (y_1 + iy_2)^{m-r} (x_1 + ix_2)^r$$

and its consequence

$$\begin{aligned} & (\Lambda_\gamma - \Lambda_1)\{(x - y) \cdot (\omega + i\omega^\perp)\}^m|_{\partial\Omega} \\ &= \sum_{r=0}^m (\omega_1 - i\omega_2)^m \binom{m}{r} (-1)^{m-r} (y_1 + iy_2)^{m-r} (\Lambda_\gamma - \Lambda_1)((x_1 + ix_2)^r|_{\partial\Omega}). \end{aligned}$$

Now assume that we have finitely many noisy data (measurements)

$$(\Lambda_\gamma - \Lambda_1)((x_1 + ix_2)^r|_{\partial\Omega}) + \epsilon_r^1(x), \quad (x_1 + ix_2)^r + \epsilon_r^2(x), \quad (2.7)$$

where $0 \leq r \leq nN$ and $\epsilon_r^1, \epsilon_r^2 \in L^2(\partial\Omega)$. Set $e^{j,nN} = (\epsilon_0^j, \dots, \epsilon_{nN}^j)$, $j = 1, 2$ and assume that

$$\|\vec{\epsilon}\| = \|(\epsilon^{1,nN}, \epsilon^{2,nN})\| \equiv \max_{j=1,2} \max_{0 \leq r \leq nN} \|\epsilon_r^j\|_{L^2(\partial\Omega)} \leq \epsilon.$$

Define the exponent

$$p(\theta/\beta, y) = 1 + \frac{n\theta e c_y^n}{\beta(c_y^n + 1)} \log(1 + |y|). \quad (2.8)$$

Let

$$\delta = \epsilon^{1/p(\theta/\beta, y)} \quad (2.9)$$

and set

$$\mathcal{E}_m^j(x) = \sum_{r=0}^m \binom{m}{r} (y_1 + iy_2)^{m-r} \epsilon_r^j(x)$$

for $j = 1, 2$. Since $[c] \leq c \leq [c] + 1$, for $N = N_\theta^\beta(\delta; y)$ from (2.5) we have

$$N \leq -\frac{\theta e c_y^n \log \delta}{\beta(c_y^n + 1)} \leq N + 1. \quad (2.10)$$

Then, from (2.8)~(2.10) one knows that $\vec{\epsilon}$ satisfies $\|\vec{\epsilon}\| \leq \delta/(1 + |y|)^{nN}$ for $N = N_\theta^\beta(\delta; y)$. This implies that \mathcal{E} satisfies (2.1). Thus we can compute $I_{(y,\omega)}^{1/n,nN}(\tau; \mathcal{E})$ from finitely many noisy data (2.7) as

$$\begin{aligned} I_{(y,\omega)}^{1/n,nN}(\tau; \mathcal{E}) &= \sum_{0 \leq m, l \leq nN} \frac{\tau^{m+l} (\omega_1 - i\omega_2)^m (\omega_1 + i\omega_2)^l}{\Gamma(\frac{m}{n} + 1) \Gamma(\frac{l}{n} + 1)} \\ &\times \sum_{r_1=0}^m \sum_{r_2=0}^l \binom{m}{r_1} \binom{l}{r_2} (-1)^{m+l-r_1-r_2} (y_1 + iy_2)^{m-r_1} (y_1 - iy_2)^{l-r_2} \quad (2.11) \\ &\times \int_{\partial\Omega} \{(\Lambda_\gamma - \Lambda_1)((x_1 + ix_2)^{r_1}|_{\partial\Omega}) + \epsilon_{r_1}^1\} \cdot \overline{\{(x_1 + ix_2)^{r_2}|_{\partial\Omega} + \epsilon_{r_2}^2\}} d\sigma. \end{aligned}$$

Then, from theorem 2.1 we immediately obtain the following.

Corollary 2.1 *Let δ be given by (2.9). Then Theorem 2.1 holds when we replace δ by ϵ and $\|\mathcal{E}\|$ by $\|\vec{\epsilon}\|$.*

Corollary 2.1 means that if ϵ is sufficiently small then for finitely many points y in Ω and directions ω the function $|I_{(y,\omega)}^{1/n,nN}(\tau_y^{1/n,\beta}(N); \mathcal{E})|$ which can be computed from finite and noisy data, plays a role of "radar".

3. Preliminaries about Mittag-Leffler's function

Mittag-Leffler's function $E_\alpha(z)$ defined in the introduction plays a central role in our analysis. In this section we present some of its properties.

It is known that $E_\alpha(z)$ has a closed form when α is rational ([1]). We will make use of this fact since for our purpose it suffices to consider only the case when $\alpha = 1/2, 1/3, \dots$. For the reader's convenience we present a direct proof.

Proposition 3.1 *Let $n \geq 2$. Then $E_{1/n}(z)$ has the form*

$$E_{1/n}(z) = e^{z^n} \left\{ 1 + n \sum_{k=1}^{n-1} \frac{1}{\Gamma(1 - \frac{k}{n})} \int_0^z e^{-u^n} u^{n-1-k} du \right\}. \quad (3.1)$$

Proof. Since

$$\int_0^1 (1-w^n)^m w^{l-1} dw = \frac{1}{n} \int_0^1 (1-s)^{(m+1)-1} s^{l/n-1} ds = \frac{1}{n} B\left(\frac{l}{n}, m+1\right),$$

we have

$$\begin{aligned} e^{z^n} \int_0^z e^{-u^n} u^{n-1-k} du &= \int_0^z e^{z^n - u^n} u^{n-1-k} du = \sum_{m=0}^{\infty} \frac{1}{m!} \int_0^z (z^n - u^n)^m u^{n-1-k} du \\ &= \sum_{m=0}^{\infty} \frac{z^{nm+n-k}}{m!} \int_0^1 (1-w^n)^m w^{n-1-k} dw = \sum_{m=0}^{\infty} \frac{z^{nm+n-k}}{m!} B\left(\frac{n-k}{n}, m+1\right) \frac{1}{n}. \end{aligned} \quad (3.2)$$

A combination of (3.2) and the formula $B(p, q) = \Gamma(p)\Gamma(q)/\Gamma(p+q)$ yields

$$\begin{aligned} n e^{z^n} \sum_{k=1}^{n-1} \frac{\int_0^z e^{-u^n} u^{n-1-k} du}{\Gamma(1 - \frac{k}{n})} &= \sum_{k=1}^{n-1} \sum_{m=0}^{\infty} \frac{z^{nm+n-k}}{m!} \frac{B(\frac{n-k}{n}, m+1)}{\Gamma(1 - \frac{k}{n})} \\ &= \sum_{k=1}^{n-1} \sum_{m=0}^{\infty} \frac{B(1 - \frac{k}{n}, m+1)}{\Gamma(m+1)\Gamma(1 - \frac{k}{n})} z^{nm+n-k} = \sum_{k=1}^{n-1} \sum_{m=0}^{\infty} \frac{z^{nm+n-k}}{\Gamma(1 - \frac{k}{n} + m+1)} \\ &= \sum_{m=0}^{\infty} \sum_{k=1}^{n-1} \frac{z^{mn+n-k}}{\Gamma(\frac{1}{n}(nm+n-k)+1)} = \sum_{m=0}^{\infty} \sum_{j=1}^{n-1} \frac{z^{nm+j}}{\Gamma(\frac{1}{n}(nm+j)+1)}. \end{aligned}$$

From this and the expansion

$$e^{z^n} = \sum_{m=0}^{\infty} \frac{z^{nm}}{\Gamma(\frac{nm}{n} + 1)}$$

one concludes that (3.1) is valid. \square

Remark 3.1. Since

$$E_{1/n}(z^{1/n}) = \sum_{m=0}^{\infty} \frac{z^{m/n}}{\Gamma(\frac{m}{n} + 1)},$$

we have

$$\begin{aligned} \frac{d}{dz}\{E_{1/n}(z^{1/n})\} &= \sum_{m=1}^{\infty} \frac{m}{n} \frac{z^{(m-n)/n}}{\Gamma(\frac{m}{n}+1)} = \sum_{m=1}^{n-1} \frac{m}{n} \frac{z^{(m-n)/n}}{\Gamma(\frac{m}{n}+1)} + \sum_{m=n}^{\infty} \frac{m}{n} \frac{z^{(m-n)/n}}{\Gamma(\frac{m}{n}+1)} \\ &= \sum_{k=1}^{n-1} \frac{n-k}{n} \frac{z^{-k/n}}{\Gamma(\frac{n-k}{n}+1)} + \sum_{m=0}^{\infty} \frac{m+n}{n} \frac{z^{m/n}}{\Gamma(\frac{m+n}{n}+1)}. \end{aligned}$$

Since

$$\Gamma(\frac{n-k}{n}+1) = \frac{n-k}{n} \Gamma(\frac{n-k}{n}), \quad \Gamma(\frac{m+n}{n}+1) = \frac{m+n}{n} \Gamma(\frac{m+n}{n}),$$

we obtain

$$\frac{d}{dz}\{E_{1/n}(z^{1/n})\} = \sum_{k=1}^{n-1} \frac{z^{-k/n}}{\Gamma(1-\frac{k}{n})} + E_{1/n}(z^{1/n}). \quad (3.3)$$

Integrating this equation, we obtain (3.1) again. This is described in [1].

Proposition 3.2. *Let $n \geq 2$ and $N \geq 1$. The truncated power series*

$$E_{1/n}^{nN}(z) = \sum_{m=0}^{nN} \frac{z^m}{\Gamma(\frac{m}{n}+1)}, \quad (3.4)$$

satisfies the following two estimates:

$$|E_{1/n}(z) - E_{1/n}^{nN}(z)| \leq \sum_{k=1}^n \frac{|z|^{nN+k}}{\Gamma(\frac{nN+k}{n})} \exp(|\operatorname{Re} z^n|). \quad (3.5)$$

$$\left| \frac{d}{dz}\{E_{1/n}(z) - E_{1/n}^{nN}(z)\} \right| \leq n|z|^{n-1} \sum_{k=1}^n \frac{|z|^{n(N-1)+k}}{\Gamma(\frac{n(N-1)+k}{n})} \exp(|\operatorname{Re} z^n|). \quad (3.6)$$

Proof. Write

$$\begin{aligned} E_{1/n}^{nN}(z) &= \sum_{m=0}^N \frac{z^{nm}}{m!} + \sum_{m=0}^{N-1} \sum_{j=1}^{n-1} \frac{z^{nm+j}}{\Gamma(\frac{nm+j}{n}+1)}; \\ E_{1/n}(z) &= \sum_{m=0}^{\infty} \frac{z^{nm}}{m!} + \sum_{m=0}^{\infty} \sum_{j=1}^{n-1} \frac{z^{nm+j}}{\Gamma(\frac{nm+j}{n}+1)}. \end{aligned}$$

Then we have the expression

$$\begin{aligned} E_{1/n}(z) - E_{1/n}^{nN}(z) &= \sum_{m>N} \frac{z^{nm}}{m!} + \sum_{m>N-1} \sum_{j=1}^{n-1} \frac{z^{nm+j}}{\Gamma(\frac{nm+j}{n}+1)} \\ &= (e^{z^n} - \sum_{m=0}^N \frac{z^{nm}}{m!}) + \sum_{k=1}^{n-1} \frac{n}{\Gamma(1-\frac{k}{n})} \int_0^z \{e^{z^n-u^n} - \sum_{m=0}^{N-1} \frac{(z^n-u^n)^m}{m!}\} u^{n-1-k} du \\ &= (e^{z^n} - \sum_{m=0}^N \frac{z^{nm}}{m!}) + \sum_{k=1}^{n-1} \frac{nz^{n-k}}{\Gamma(1-\frac{k}{n})} \int_0^1 \{e^{z^n(1-w^n)} - \sum_{m=0}^{N-1} \frac{\{z^n(1-w^n)\}^m}{m!}\} w^{n-1-k} dw. \end{aligned} \quad (3.7)$$

Using the inequality

$$\left| e^z - \sum_{m=0}^N \frac{z^m}{m!} \right| \leq \frac{|z|^{N+1} e^{|\operatorname{Re} z|}}{(N+1)!}, \quad (3.8)$$

we see that

$$\begin{aligned} & \left| \sum_{k=1}^{n-1} \frac{nz^{n-k}}{\Gamma(1-\frac{k}{n})} \int_0^1 \{e^{z^n(1-w^n)} - \sum_{m=0}^{N-1} \frac{\{z^n(1-w^n)\}^m}{m!}\} w^{n-1-k} dw \right| \\ & \leq \sum_{k=1}^{n-1} \frac{n|z|^{n-k}}{\Gamma(1-\frac{k}{n})} \int_0^1 \frac{|z^n(1-w^n)|^N}{N!} e^{|\operatorname{Re} z^n(1-w^n)|} w^{n-1-k} dw \\ & \leq \sum_{k=1}^{n-1} \frac{n|z|^{n-k+nN} e^{|\operatorname{Re} z^n|}}{N! \Gamma(1-\frac{k}{n})} \int_0^1 (1-w^n)^N w^{n-1-k} dw \\ & = \sum_{k=1}^{n-1} \frac{n|z|^{n-k+nN} e^{|\operatorname{Re} z^n|}}{\Gamma(N+1) \Gamma(1-\frac{k}{n})} B\left(\frac{n-k}{n}, N+1\right) \frac{1}{n} \\ & = \sum_{k=1}^{n-1} \frac{|z|^{n-k+nN} e^{|\operatorname{Re} z^n|}}{\Gamma(\frac{n-k+nN}{n} + 1)} = \sum_{k=1}^{n-1} \frac{|z|^{k+nN} e^{|\operatorname{Re} z^n|}}{\Gamma(\frac{k+nN}{n} + 1)}. \end{aligned} \quad (3.9)$$

From (3.7)~(3.9) we obtain (3.5). From (3.7) we have

$$\begin{aligned} \frac{d}{dz} \{E_{1/n}(z) - E_{1/n}^{nN}(z)\} &= \frac{d}{dz} \left\{ e^{z^n} - \sum_{m=0}^N \frac{z^{nm}}{m!} \right\} \\ &+ \sum_{k=1}^{n-1} \frac{n}{\Gamma(1-\frac{k}{n})} \int_0^z \frac{d}{dz} \left\{ e^{z^n-u^n} - \sum_{m=0}^{N-1} \frac{(z^n-u^n)^m}{m!} \right\} u^{n-1-k} du \\ &= nz^{n-1} \left\{ e^{z^n} - \sum_{m=1}^N \frac{z^{n(m-1)}}{(m-1)!} \right\} \\ &+ nz^{n-1} \sum_{k=1}^{n-1} \frac{n}{\Gamma(1-\frac{k}{n})} \int_0^z \left\{ e^{z^n-u^n} - \sum_{m=1}^{N-1} \frac{(z^n-u^n)^{m-1}}{(m-1)!} \right\} u^{n-1-k} du \\ &= nz^{n-1} \left\{ e^{z^n} - \sum_{m=0}^{N-1} \frac{z^{nm}}{m!} \right\} \\ &+ nz^{n-1} \sum_{k=1}^{n-1} \frac{n}{\Gamma(1-\frac{k}{n})} \int_0^z \left\{ e^{z^n-u^n} - \sum_{m=0}^{N-2} \frac{(z^n-u^n)^m}{m!} \right\} u^{n-1-k} du, \end{aligned}$$

and this yields

$$\frac{d}{dz} \{E_{1/n}(z) - E_{1/n}^{nN}(z)\} = nz^{n-1} \{E_{1/n}(z) - E_{1/n}^{n(N-1)}(z)\}. \quad (3.10)$$

From (3.5) and (3.10) we obtain (3.6). \square

Remark 3.2. It is easy to see that the function $e^{z^n} - \sum_{m=0}^N \frac{z^{nm}}{m!}$ satisfies

$$\frac{d}{dz} \left\{ e^{z^n} - \sum_{m=0}^N \frac{z^{nm}}{m!} \right\} = nz^{n-1} \left\{ e^{z^n} - \sum_{m=0}^{N-1} \frac{z^{nm}}{m!} \right\}.$$

Therefore both $e^{z^n} - \sum_{m=0}^N \frac{z^{nm}}{m!}$ and $E_{1/n}(z) - E_{1/n}^N(z)$ satisfy the recurrence formula

$$\frac{d}{dz} \Psi_N(z; n) = nz^{n-1} \Psi_{N-1}(z; n).$$

Proposition 3.3. Let $n \geq 2$ and $N \geq 1$. Mittag-Leffler's function and its truncated power series satisfy the following estimates:

$$|E_{1/n}(z)| \leq \sum_{k=0}^{n-1} \frac{|z|^k}{\Gamma(\frac{k}{n} + 1)} e^{|\operatorname{Re} z^n|.} \quad (3.11)$$

$$\left| \frac{d}{dz} E_{1/n}(z) \right| \leq n \sum_{k=0}^{2(n-1)} \frac{|z|^k}{\Gamma(\frac{k+1}{n})} e^{|\operatorname{Re} z^n|.} \quad (3.12)$$

$$|E_{1/n}^N(z)| \leq \sum_{k=0}^{n-1} \frac{|z|^k}{\Gamma(\frac{k}{n} + 1)} e^{|z|^n}. \quad (3.13)$$

$$\left| \frac{d}{dz} E_{1/n}^N(z) \right| \leq n \sum_{k=0}^{2(n-1)} \frac{|z|^k}{\Gamma(\frac{k+1}{n})} e^{|z|^n}. \quad (3.14)$$

Proof. From (3.1) one has

$$E_{1/n}(z) = e^{z^n} + n \sum_{k=1}^{n-1} \frac{z^{n-k}}{\Gamma(1 - \frac{k}{n})} \int_0^1 e^{z^n(1-w^n)} w^{n-1-k} dw.$$

This yields (3.11) as indicated below:

$$\begin{aligned} |E_{1/n}(z)| &\leq e^{|\operatorname{Re} z^n|} + n \sum_{k=1}^{n-1} \frac{|z|^{n-k}}{\Gamma(1 - \frac{k}{n})} e^{|\operatorname{Re} z^n|} \int_0^1 w^{n-1-k} dw \\ &= e^{|\operatorname{Re} z^n|} \left\{ 1 + n \sum_{k=1}^{n-1} \frac{|z|^{n-k}}{\Gamma(1 - \frac{k}{n})(n-k)} \right\} \\ &= e^{|\operatorname{Re} z^n|} \left\{ 1 + \sum_{k=1}^{n-1} \frac{|z|^{n-k}}{\Gamma(1 - \frac{k}{n})(1 - \frac{k}{n})} \right\} \\ &= e^{|\operatorname{Re} z^n|} \left\{ 1 + \sum_{k=1}^{n-1} \frac{|z|^{n-k}}{\Gamma(1 - \frac{k}{n} + 1)} \right\} = e^{|\operatorname{Re} z^n|} \left\{ 1 + \sum_{k=1}^{n-1} \frac{|z|^{n-k}}{\Gamma(\frac{n-k}{n} + 1)} \right\} \\ &= e^{|\operatorname{Re} z^n|} \left\{ 1 + \sum_{k=1}^{n-1} \frac{|z|^k}{\Gamma(\frac{k}{n} + 1)} \right\} = e^{|\operatorname{Re} z^n|} \sum_{k=0}^{n-1} \frac{|z|^k}{\Gamma(\frac{k}{n} + 1)}. \end{aligned}$$

From (3.3) we have

$$\frac{d}{dz}E_{1/n}(z) = nz^{n-1}\left\{\sum_{k=1}^{n-1}\frac{z^{-k}}{\Gamma(1-\frac{k}{n})} + E_{1/n}(z)\right\} = n\sum_{k=0}^{n-2}\frac{z^k}{\Gamma(\frac{k+1}{n})} + nz^{n-1}E_{1/n}(z).$$

This and (3.11) yields (3.12) as indicated below:

$$\begin{aligned} \left|\frac{d}{dz}E_{1/n}(z)\right| &\leq n\left\{\sum_{k=0}^{n-2}\frac{|z|^k}{\Gamma(\frac{k+1}{n})} + \sum_{k=0}^{n-1}\frac{|z|^{n-1+k}}{\Gamma(\frac{k}{n}+1)}e^{|\operatorname{Re} z^n|}\right\} \\ &= n\left\{\sum_{k=0}^{n-2}\frac{|z|^k}{\Gamma(\frac{k+1}{n})} + \sum_{k=n-1}^{2(n-1)}\frac{|z|^k}{\Gamma(\frac{k+1}{n})}e^{|\operatorname{Re} z^n|}\right\} \\ &\leq n\sum_{k=0}^{2(n-1)}\frac{|z|^k}{\Gamma(\frac{k+1}{n})}e^{|\operatorname{Re} z^n|}. \end{aligned}$$

It is easy to see that

$$\begin{aligned} |E_{1/n}^{nN}(z)| &\leq E_{1/n}^{nN}(|z|) \leq E_{1/n}(|z|), \\ \left|\frac{d}{dz}E_{1/n}^{nN}(z)\right| &\leq \frac{d}{d|z|}E_{1/n}^{nN}(|z|) \leq \frac{d}{d|z|}E_{1/n}(|z|). \end{aligned}$$

Thus (3.11) and (3.12) yield (3.13) and (3.14). \square

4. Truncated indicator function

In this section we introduce a truncation of the indicator function (given in Definition 1.2) that can be computed from finite data. Further, we use the properties of Mittag-Leffler's function to analyze the asymptotic behavior of the truncation.

Definition 4.1 Let $N \geq 1$. Define the *truncated indicator function* by

$$\begin{aligned} I_{(y,\omega)}^{1/n,nN}(\tau) &= \int_{\partial\Omega} (\Lambda_\gamma - \Lambda_1)g \cdot \bar{g}d\sigma, \\ g(x) &= E_{1/n}^{nN}(\tau\{(x-y) \cdot (\omega + i\omega^\perp)\}), \quad x \in \partial\Omega, \end{aligned}$$

where $E_{1/n}^{nN}(z)$ is defined by equation (3.4).

Proposition 4.1 Let $n \geq 2$ and $N \geq 1$. Let β_0 be the unique positive solution of equation (2.3). Given $\beta \in]0, \beta_0[$ we have

$$\lim_{N \rightarrow \infty} |I_{(y,\omega)}^{1/n}(\tau_y^{1/n,\beta}(N)) - I_{(y,\omega)}^{1/n,nN}(\tau_y^{1/n,\beta}(N))| = 0.$$

The convergence is uniform with respect to ω .

Proof. Given $(y,\omega) \in \Omega \times S^1$ set $z = \tau\{(x-y) \cdot (\omega + i\omega^\perp)\}$, $\tau > 0$. Then for any $x \in \Omega$ we have $|z| = \tau|x-y| \leq \tau c_y$. From (3.5) and (3.6) we get

$$\begin{aligned} \|E_{1/n} - E_{1/n}^{nN}\|_{L^2(\Omega)} &\leq |\Omega|^{1/2} \sum_{k=1}^n \frac{(\tau c_y)^{nN+k}}{\Gamma(\frac{nN+k}{n})} e^{(\tau c_y)^n}, \\ \|\nabla\{E_{1/n} - E_{1/n}^{nN}\}\|_{L^2(\Omega)} &\leq |\Omega|^{1/2} \sqrt{2}n\tau(\tau c_y)^{n-1} \sum_{k=1}^n \frac{(\tau c_y)^{n(N-1)+k}}{\Gamma(\frac{n(N-1)+k}{n})} e^{(\tau c_y)^n}. \end{aligned}$$

Let $C > 0$ satisfy

$$\|v|_{\partial\Omega}\|_{H^{1/2}(\partial\Omega)} \leq C\|v\|_{H^1(\Omega)} \quad \forall v \in H^1(\Omega). \quad (4.1)$$

From the inequalities described above and (4.1) we obtain

$$\begin{aligned} & \|E_{1/n}(z) - E_{1/n}^{nN}(z)\|_{H^{1/2}(\partial\Omega)} \leq C|\Omega|^{1/2}e^{(\tau c_y)^n} \\ & \times \sqrt{\left\{ \sum_{k=1}^n \frac{(\tau c_y)^{nN+k}}{\Gamma(\frac{nN+k}{n})} \right\}^2 + \left\{ \sqrt{2}n\tau(\tau c_y)^{n-1} \sum_{k=1}^n \frac{(\tau c_y)^{n(N-1)+k}}{\Gamma(\frac{n(N-1)+k}{n})} \right\}^2}. \end{aligned} \quad (4.2)$$

From (3.11) and (3.12) we get

$$\begin{aligned} \|E_{1/n}(z)\|_{L^2(\Omega)} & \leq |\Omega|^{1/2} \sum_{k=0}^{n-1} \frac{(\tau c_y)^k}{\Gamma(\frac{k}{n} + 1)} e^{(\tau c_y)^n}, \\ \|\nabla E_{1/n}(z)\|_{L^2(\Omega)} & \leq |\Omega|^{1/2} \sqrt{2}n\tau \sum_{k=0}^{2(n-1)} \frac{(\tau c_y)^k}{\Gamma(\frac{k+1}{n})} e^{(\tau c_y)^n}. \end{aligned}$$

From these and (4.1) we obtain

$$\|E_{1/n}\|_{H^{1/2}(\partial\Omega)} \leq C|\Omega|^{1/2}e^{(\tau c_y)^n} \sqrt{\left\{ \sum_{k=0}^{n-1} \frac{(\tau c_y)^k}{\Gamma(\frac{k}{n} + 1)} \right\}^2 + \left\{ \sqrt{2}n\tau \sum_{k=0}^{2(n-1)} \frac{(\tau c_y)^k}{\Gamma(\frac{k+1}{n})} \right\}^2}. \quad (4.3)$$

Recall the infinite-data indicator function

$$I_{(y,\omega)}^{1/n}(\tau) = \int_{\partial\Omega} (\Lambda_\gamma - \Lambda_1) f \cdot \bar{f} d\sigma, \quad f(x) = E_{1/n}(\tau\{(x-y) \cdot (\omega + i\omega^\perp)\}).$$

Since

$$\begin{aligned} & I_{(y,\omega)}^{1/n}(\tau) - I_{(y,\omega)}^{1/n,nN}(\tau) \\ & = \int_{\partial\Omega} (\Lambda_\gamma - \Lambda_1) f \cdot \bar{f} d\sigma - \int_{\partial\Omega} (\Lambda_\gamma - \Lambda_1) \{f + (g-f)\} \cdot \overline{\{f + (g-f)\}} d\sigma \\ & = \int_{\partial\Omega} \left((\Lambda_\gamma - \Lambda_1) f \cdot \overline{(f-g)} + (\Lambda_\gamma - \Lambda_1)(f-g) \cdot \bar{f} - (\Lambda_\gamma - \Lambda_1)(f-g) \cdot \overline{(f-g)} \right) d\sigma, \end{aligned}$$

from (4.2) and (4.3) we obtain

$$\begin{aligned} & |I_{(y,\omega)}^{1/n}(\tau) - I_{(y,\omega)}^{1/n,nN}(\tau)| \\ & \leq \|\Lambda_\gamma - \Lambda_1\|_{1/2,-1/2} \|f - g\|_{H^{1/2}(\partial\Omega)} (2\|f\|_{H^{1/2}(\partial\Omega)} + \|f - g\|_{H^{1/2}(\partial\Omega)}) \\ & \leq C^2 |\Omega| \|\Lambda_\gamma - \Lambda_1\|_{1/2,-1/2} e^{2(\tau c_y)^n} \end{aligned}$$

$$\begin{aligned}
& \times \sqrt{\left\{ \sum_{k=1}^n \frac{(\tau c_y)^{nN+k}}{\Gamma(\frac{nN+k}{n})} \right\}^2 + \left\{ \sqrt{2}n\tau(\tau c_y)^{n-1} \sum_{k=1}^n \frac{(\tau c_y)^{n(N-1)+k}}{\Gamma(\frac{n(N-1)+k}{n})} \right\}^2} \\
& \times \sqrt{\left\{ \sum_{k=0}^{n-1} \frac{(\tau c_y)^k}{\Gamma(\frac{k}{n} + 1)} \right\}^2 + \left\{ \sqrt{2}n\tau \sum_{k=0}^{2(n-1)} \frac{(\tau c_y)^k}{\Gamma(\frac{k+1}{n})} \right\}^2} \\
& + \sqrt{\left\{ \sum_{k=1}^n \frac{(\tau c_y)^{nN+k}}{\Gamma(\frac{nN+k}{n})} \right\}^2 + \left\{ \sqrt{2}n\tau(\tau c_y)^{n-1} \sum_{k=1}^n \frac{(\tau c_y)^{n(N-1)+k}}{\Gamma(\frac{n(N-1)+k}{n})} \right\}^2}.
\end{aligned} \tag{4.4}$$

Define $K(\beta) = -(2\beta/e + \log \beta) > 0$ and set $\tau = \tau_y^{1/n, \beta}(N)$. Since $\tau \sim N^{1/n}$ and

$$\Gamma(N + \frac{1}{n}) \sim \left(\frac{N + \frac{1}{n}}{e}\right)^{N + \frac{1}{n}} \sqrt{\frac{2\pi}{N + \frac{1}{n}}}$$

as $N \rightarrow \infty$, it is easy to see that

$$\begin{aligned}
& e^{2(\tau c_y)^n} \sqrt{\left\{ \sum_{k=1}^n \frac{(\tau c_y)^{nN+k}}{\Gamma(\frac{nN+k}{n})} \right\}^2 + \left\{ \sqrt{2}n\tau(\tau c_y)^{n-1} \sum_{k=1}^n \frac{(\tau c_y)^{n(N-1)+k}}{\Gamma(\frac{n(N-1)+k}{n})} \right\}^2} \\
& \sim e^{2(\tau c_y)^n} \frac{\tau^{2n} (\tau c_y)^{nN}}{\Gamma(N + \frac{1}{n})} \sim e^{2(\tau c_y)^n} N^{2+\frac{1}{2}} (\tau c_y)^{nN} \left(\frac{e}{N + \frac{1}{n}}\right)^{N + \frac{1}{n}} \\
& = e^{2(\tau c_y)^n} N^{5/2} \exp\left\{n\left(N + \frac{1}{n}\right) \log(\tau c_y) - \log(\tau c_y) + \left(N + \frac{1}{n}\right) \log \frac{e}{N + \frac{1}{n}}\right\} \\
& = \frac{N^{5/2}}{\tau c_y} \exp\left\{2(\tau c_y)^n + \left(N + \frac{1}{n}\right) \log \frac{e(\tau c_y)^n}{N + \frac{1}{n}}\right\} \sim N^{\frac{5}{2} - \frac{1}{n}} e^{-(N + \frac{1}{n})K(\beta)}.
\end{aligned}$$

From this, (4.4) and a simple observation we obtain the convergence rate

$$|I_{(y, \omega)}^{1/n}(\tau, t) - I_{(y, \omega)}^{1/n, nN}(\tau, t)| = O(N^{\frac{5}{2} - \frac{1}{n} + 2 - \frac{1}{n}} e^{-(N + \frac{1}{n})K(\beta)}).$$

□

Now the next theorem is a direct consequence of Theorem 1.1 and Proposition 4.1.

Theorem 4.1 *Let $n \geq 2$, $\alpha = 1/n$ and $N \geq 1$. We have:*

if $\{C_y(\omega, \pi\alpha/2)\} \cap \overline{D} = \emptyset$, then

$$\lim_{N \rightarrow \infty} |I_{(y, \omega)}^{1/n, nN}(\tau_y^{1/n, \beta}(N))| = 0;$$

if $\{C_y(\omega, \pi\alpha/2)\} \cap \overline{D} \neq \emptyset$ and $C_y(\omega, \pi\alpha/2) \cap D = \emptyset$, then

$$\liminf_{N \rightarrow \infty} |I_{(y, \omega)}^{1/n, nN}(\tau_y^{1/n, \beta}(N))| > 0;$$

if $C_y(\omega, \pi\alpha/2) \cap D \neq \emptyset$, then

$$\lim_{N \rightarrow \infty} |I_{(y, \omega)}^{1/n, nN}(\tau_y^{1/n, \beta}(N))| = \infty.$$

5. Truncated indicator function and noisy data

In this section we study the relationship between the noisy truncated indicator function (see definition 2.1) and the truncated indicator function (see definition 4.1). Write

$$I_{(y,\omega)}^{1/n,nN}(\tau; \mathcal{E}) = \int_{\partial\Omega} \{(\Lambda_\gamma - \Lambda_1)(E_{1/n}^{nN}(\tau\{(x-y) \cdot (\omega + i\omega^\perp)\}))|_{\partial\Omega}\} + \sum_{m=0}^{nN} \frac{\tau^m \mathcal{E}_m^1(x)}{\Gamma(\frac{m}{n} + 1)} \cdot \overline{\{E_{1/n}^{nN}(\tau\{(x-y) \cdot (\omega + i\omega^\perp)\}) + \sum_{l=0}^{nN} \frac{\tau^l}{\Gamma(\frac{l}{n} + 1)} \mathcal{E}_l^2(x)\}} d\sigma(x).$$

We can estimate the difference between the truncated indicator functions as follows.

Proposition 5.1 *Let $n \geq 2$. Given $\beta \in]0, \beta_0[$ and $\theta \in]0, 1[$ let δ satisfy (2.4). For $N = N_\theta^\beta(\delta; y)$ given by (2.5) we have*

$$\sup_{\|\mathcal{E}\| \leq \delta} |I_{(y,\omega)}^{1/n,nN}(\tau_y^{1/n,\beta}(N); \mathcal{E}) - I_{(y,\omega)}^{1/n,nN}(\tau_y^{1/n,\beta}(N))| = O(\delta^{1-\theta} |\log \delta|^{(2n-1)/n})$$

as $\delta \rightarrow 0$. The convergence is uniform with respect to ω .

Proof. Write

$$\begin{aligned} I_{(y,\omega)}^{1/n,nN}(\tau; \mathcal{E}) - I_{(y,\omega)}^{1/n,nN}(\tau) &= \int_{\partial\Omega} \sum_{m=0}^{nN} \frac{\tau^m \mathcal{E}_m^1(x)}{\Gamma(\frac{m}{n} + 1)} \cdot \overline{\sum_{\ell=0}^{nN} \frac{\tau^\ell \mathcal{E}_\ell^2(x)}{\Gamma(\frac{\ell}{n} + 1)}} d\sigma(x) \\ &+ \int_{\partial\Omega} (\Lambda_\gamma - \Lambda_1)(E_{1/n}^{nN}(\tau\{(x-y) \cdot (\omega + i\omega^\perp)\}))|_{\partial\Omega} \cdot \overline{\sum_{\ell=0}^{nN} \frac{\tau^\ell \mathcal{E}_\ell^2(x)}{\Gamma(\frac{\ell}{n} + 1)}} d\sigma(x) \quad (5.1) \\ &+ \int_{\partial\Omega} \sum_{m=0}^{nN} \frac{\tau^m \mathcal{E}_m^1(x)}{\Gamma(\frac{m}{n} + 1)} \cdot \overline{E_{1/n}^{nN}(\tau\{(x-y) \cdot (\omega + i\omega^\perp)\})} d\sigma(x). \end{aligned}$$

Let $z = \tau(x-y) \cdot (\omega + i\omega^\perp)$. From (3.13) and (3.14) we have :

$$\begin{aligned} \|E_{1/n}^{nN}(z)\|_{L^2(\Omega)} &\leq |\Omega|^{1/2} \sum_{k=0}^{n-1} \frac{(\tau C_y)^k}{\Gamma(\frac{k}{n} + 1)} e^{(\tau C_y)^n}; \\ \|\nabla E_{1/n}^{nN}(z)\|_{L^2(\Omega)} &\leq |\Omega|^{1/2} \sqrt{2} n \tau \sum_{k=0}^{2(n-1)} \frac{(\tau C_y)^k}{\Gamma(\frac{k+1}{n})} e^{(\tau C_y)^n}. \end{aligned}$$

From these and (4.1) we have

$$\|E_{1/n}^{nN}\|_{H^{1/2}(\partial\Omega)} \leq C |\Omega|^{1/2} e^{(\tau C_y)^n} \sqrt{\left\{ \sum_{k=0}^{n-1} \frac{(\tau C_y)^k}{\Gamma(\frac{k}{n} + 1)} \right\}^2 + \left\{ \sqrt{2} n \tau \sum_{k=0}^{2(n-1)} \frac{(\tau C_y)^k}{\Gamma(\frac{k+1}{n})} \right\}^2}. \quad (5.2)$$

From (2.1), (5.1) and (5.2) we obtain

$$\begin{aligned}
|I_{(y,\omega)}^{1/n,nN}(\tau; \mathcal{E}) - I_{(y,\omega)}^{1/n,nN}(\tau)| &\leq \sum_{m=0}^{nN} \frac{\tau^m \|\mathcal{E}_m^1\|_{L^2(\partial\Omega)}}{\Gamma(\frac{m}{n} + 1)} \sum_{\ell=0}^{nN} \frac{\tau^\ell \|\mathcal{E}_\ell^2\|_{L^2(\partial\Omega)}}{\Gamma(\frac{\ell}{n} + 1)} \\
&+ \|\Lambda_\gamma - \Lambda_1\|_{\frac{1}{2},0} \|E_{1/n}^{nN}(\tau\{(x-y) \cdot (\omega + i\omega^\perp)\})\|_{H^{1/2}(\partial\Omega)} \sum_{l=0}^{nN} \frac{\tau^l \|\mathcal{E}_l^2\|_{L^2(\partial\Omega)}}{\Gamma(\frac{l}{n} + 1)} \\
&+ \sum_{m=0}^{nN} \frac{\tau^m \|\mathcal{E}_m^1\|_{L^2(\partial\Omega)}}{\Gamma(\frac{m}{n} + 1)} \|E_{1/n}^{nN}(\tau\{(x-y) \cdot (\omega + i\omega^\perp)\})\|_{H^{1/2}(\partial\Omega)} \\
&\leq C|\Omega|^{1/2} (\|\Lambda_\gamma - \Lambda_1\|_{1/2,0} + 1) e^{(\tau C_y)^n} E_{1/n}(\tau) \delta \\
&\quad \times \sqrt{\left\{ \sum_{k=0}^{n-1} \frac{(\tau C_y)^k}{\Gamma(\frac{k}{n} + 1)} \right\}^2 + \left\{ \sqrt{2} n \tau \sum_{k=0}^{2(n-1)} \frac{(\tau C_y)^k}{\Gamma(\frac{k+1}{n})} \right\}^2 + \{e^{(\tau C_y)^n} E_{1/n}(\tau) \delta\}^2}.
\end{aligned} \tag{5.3}$$

Note that we have made use of a regularity result at the boundary $\|\Lambda_\gamma - \Lambda_1\|_{1/2,0} < \infty$.

Formula (2.4) ensures $N_\theta^\beta(\delta; y) \geq 1$. (2.10) yields, for $\tau = \tau_y^{1/n,\beta}(N)$

$$\tau^n \leq -\frac{\theta \log \delta}{C_y^n + 1} + \frac{\beta}{enC_y^n} \leq \tau^n + \frac{\beta}{eC_y^n}. \tag{5.4}$$

Since $E_{1/n}(\tau) \sim n e^{\tau^n}$ as $\tau \rightarrow \infty$ (see [1]), from (5.4) we obtain

$$e^{(\tau C_y)^n} E_{1/n}(\tau) \delta = O(\delta^{1-\theta}) \tag{5.5}$$

as $\delta \rightarrow 0$. It is easy to see that

$$\sqrt{\left\{ \sum_{k=0}^{n-1} \frac{(\tau C_y)^k}{\Gamma(\frac{k}{n} + 1)} \right\}^2 + \left\{ \sqrt{2} n \tau \sum_{k=0}^{2(n-1)} \frac{(\tau C_y)^k}{\Gamma(\frac{k+1}{n})} \right\}^2} = O(\tau^{2n-1}) = O(|\log \delta|^{(2n-1)/n}) \tag{5.6}$$

and

$$e^{-2(\tau C_y)^n} = O(\delta^{2C_y^n \theta / (C_y^n + 1)}). \tag{5.7}$$

From (5.5) and (5.7) we have

$$\{e^{(\tau C_y)^n} E_{1/n}(\tau) \delta\}^2 e^{-2(\tau C_y)^n} = O(\delta^\kappa) \tag{5.8}$$

where $\kappa = 2\{1 - \theta / (C_y^n + 1)\}$. Since $\kappa > 1 - \theta$, from (5.3), (5.5), (5.6) and (5.8) we have the desired conclusion. \square

6. The Neumann-to-Dirichlet map

In the previous sections we considered the Dirichlet-to-Neumann map Λ_γ . However, for application to EIT it is better to use the Neumann-to-Dirichlet map and establish the corresponding results. This is because in practice currents are applied and voltages measured.

In this section we assume that $\partial\Omega$ is Lipschitz. Given $g \in L^2(\partial\Omega)$ with

$$\int_{\partial\Omega} g d\sigma = 0 \quad (6.1)$$

there exists a solution $u \in H^1(\Omega)$ of the elliptic Neumann problem

$$\nabla \cdot \gamma \nabla u = 0 \text{ in } \Omega, \quad \gamma \frac{\partial u}{\partial \nu} = g \text{ on } \partial\Omega. \quad (6.2)$$

The solution u is unique up to a constant, and the function

$$R_\gamma(g) = u|_{\partial\Omega} - \frac{1}{|\partial\Omega|} \int_{\partial\Omega} u d\sigma$$

is well-defined as an element of $L^2(\partial\Omega)$. The correspondence $R_\gamma : g \mapsto R_\gamma g$ is called the Neumann-to-Dirichlet map.

We give some remarks about previous results without proofs.

(1) Theorem 1.1 is still valid under the change of the indicator function as

$$I_{(y,\omega)}^\alpha(\tau, t) = \int_{\partial\Omega} \overline{\frac{\partial e^\alpha(\cdot; y, \omega)}{\partial \nu}|_{\partial\Omega}} \cdot (R_1 - R_\gamma) \left(\frac{\partial e^\alpha(\cdot; y, \omega)}{\partial \nu} \Big|_{\partial\Omega} \right) d\sigma.$$

(2) Theorem 2.1 is valid under the change

$$\begin{aligned} I_{(y,\omega)}^{1/n, nN}(\tau; \mathcal{E}) &= \sum_{1 \leq m, l \leq nN} \frac{\tau^{m+l}}{\Gamma(\frac{m}{n} + 1) \Gamma(\frac{l}{n} + 1)} \\ &\times \int_{\partial\Omega} \overline{\left\{ \frac{\partial}{\partial \nu(x)} \{ (x-y) \cdot (\omega + i\omega^\perp) \}^l + \mathcal{E}_l^2(x) \right\}} \\ &\cdot \{ (R_1 - R_\gamma) \left(\frac{\partial}{\partial \nu(x)} \{ (x-y) \cdot (\omega + i\omega^\perp) \}^m \Big|_{\partial\Omega} \right) + \mathcal{E}_m^1(x) \} d\sigma(x). \end{aligned}$$

(3) Corollary 2.1 is valid under the change of (2.11)

$$\begin{aligned} I_{(y,\omega)}^{1/n, nN}(\tau; \mathcal{E}) &= \sum_{1 \leq m, l \leq nN} \frac{\tau^{m+l}}{\Gamma(\frac{m}{n} + 1) \Gamma(\frac{l}{n} + 1)} (\omega_1 - i\omega_2)^m (\omega_1 + i\omega_2)^l \\ &\times \sum_{r_1=0}^m \sum_{r_2=0}^l \binom{m}{r_1} \binom{l}{r_2} (-1)^{m+l-r_1-r_2} (y_1 + iy_2)^{m-r_1} (y_1 - iy_2)^{l-r_2} \\ &\times \int_{\partial\Omega} \overline{\left\{ \frac{\partial}{\partial \nu} (x_1 + ix_2)^{r_2} \Big|_{\partial\Omega} + \epsilon_{r_2}^2(x) \right\}} \cdot \{ (R_1 - R_\gamma) \left(\frac{\partial}{\partial \nu} (x_1 + ix_2)^{r_1} \Big|_{\partial\Omega} \right) + \epsilon_{r_1}^1(x) \} d\sigma. \end{aligned} \quad (6.3)$$

We consider the special case when Ω is the unit disc. We represent the ND map as a $nN \times nN$ complex matrix defined as follows. Denote the trigonometric basis functions on $\partial\Omega$ by

$$\phi_k = (2\pi)^{-1/2} (x_1 + ix_2)^k \Big|_{\partial\Omega}, \quad k \in \mathbb{Z}.$$

We solve the Neumann problem

$$\nabla \cdot \gamma \nabla u_k = 0 \text{ in } \Omega, \quad \gamma \frac{\partial u_k}{\partial \nu} = \phi_k \text{ on } \partial\Omega, \quad (6.4)$$

for $k = 1, \dots, nN$, and set

$$\mathcal{R}_\gamma^{nN}[\ell, k] = \int_{\partial\Omega} u_k \overline{\phi_\ell} d\sigma,$$

where ℓ is row index and k is column index. We can now express (6.3) with $\epsilon_k^1 = \epsilon_k^2 = 0$ in terms of \mathcal{R}_γ^{nN} :

$$\begin{aligned} I_{(y,\omega)}^{1/n,nN}(\tau) &= 2\pi \sum_{1 \leq m, \ell \leq nN} \frac{\tau^{m+\ell} \overline{\omega^m} \omega^\ell}{\Gamma(\frac{m}{n} + 1) \Gamma(\frac{\ell}{n} + 1)} \\ &\times \sum_{r_1=1}^m \sum_{r_2=1}^\ell \binom{m}{r_1} \binom{\ell}{r_2} r_1 r_2 (-1)^{m+\ell-r_1-r_2} y^{m-r_1} \overline{y^{\ell-r_2}} \\ &\times (\mathcal{R}_1^{nN}[r_2, r_1] - \mathcal{R}_\gamma^{nN}[r_2, r_1]), \end{aligned} \quad (6.6)$$

where we use the complex notation $y = (y_1 + iy_2)$ and $\omega = (\omega_1 + i\omega_2)$.

7. Reconstruction algorithms

The truncated indicator function contains extensive knowledge about the unknown inclusion, as proved above. But how to extract that information numerically to produce a reconstruction of the inclusion D ? We present in this section two reconstruction methods. The first method makes use of the size of indicator function similarly to numerical implementations of the enclosure method and certain methods used in inverse obstacle scattering. The second method uses local minima (with respect to ω) of the indicator function.

We start by discretizing the indicator function. For $K, M > 0$, choose a finite collection of points $y_1, \dots, y_K \in \Omega$ and a discretization of the direction variable ω :

$$\omega_m = \exp(i \frac{2\pi m}{M}), \quad m = 1, \dots, M. \quad (7.1)$$

Given $n \geq 2$ and $N \geq 1$, we use (6.3) to compute the function

$$I(k, m) = \left| I_{(y_k, \omega_m)}^{1/n, nN}(\tau_k; \mathcal{E}) \right| \quad (7.2)$$

for $k = 1, \dots, K$, $m = 1, \dots, M$ and $\tau_k > 0$ chosen as explained below. We call the cones $C_{y_k}(\omega_m, \frac{\pi}{2n})$ used in the computation of $I(k, m)$ the *analyzing cones*.

We discuss the choices of $N > 0$ and τ_k in (7.2) for fixed Ω and given number of electrodes. In formula (6.3), the applied boundary current is

$$\frac{\partial}{\partial \nu} (x_1 + ix_2)^{r_1}.$$

Thus the number L of electrodes on $\partial\Omega$ gives an upper bound for r_1 , say $r_1 \leq R_1$, since very oscillatory boundary conditions cannot be expressed using electrodes. Further,

from (6.3) we see that $N \leq R_1/n$. In the definition of the truncated indicator function we use the truncated power series

$$E_{1/n}^{nN}(z) = \sum_{\ell=0}^{nN} \frac{z^\ell}{\Gamma(\frac{\ell}{n} + 1)}.$$

The difference between exact and truncated indicator function depends on the difference $|E_{1/n}(z) - E_{1/n}^{nN}(z)|$, which is small only for z close to zero. Let us assume that the difference is small enough if $|z| \leq \rho$ (a suitable value for $\rho > 0$ should be found for a given application). From Definition 1.2 and formula (1.2) we see that when computing the exact indicator function we evaluate Mittag-Leffler's function $E_{1/n}(z)$ at the argument point

$$z = \tau_k \{(x - y_k) \cdot (\omega_m + i\omega_m^\perp)\}, \quad x \in \partial\Omega.$$

To ensure accuracy of the truncated indicator function we require $|z| \leq \rho$, or

$$\tau_k \leq \frac{\rho}{|y_k| + \max_{\partial\Omega} |x|}. \quad (7.3)$$

In particular, let us consider the case when Ω is the unit disc, $n = 2$, and the number of electrodes is $L = 32$. Parametrize the boundary by

$$\partial\Omega = \{(\cos \theta, \sin \theta) : 0 \leq \theta < 2\pi\}.$$

Then the maximum spatial frequency we can (approximately) express with the electrodes at the boundary is $\exp(iL\theta/2)$. Thus $R_1 = L/2 = 16$ and we take the maximal choice $N = 8$. Based on formula (7.3), we choose

$$\tau_k = \frac{\rho}{1 + |y_k|}. \quad (7.4)$$

7.1. Reconstruction method A

We follow an idea proved successful in the context of inverse scattering (see e.g. [30, p.201]). Choose a threshold $\eta > 0$. For a fixed direction ω_m , denote

$$S_m = \bigcup_{I(k,m) > \eta} C_{y_k}(\omega_m, \frac{\pi}{2n}).$$

Since the indicator function assigns a large value to the cones included in S_m , we assume that $D \subset S_m$. Then an approximation to D is achieved as $\cap_{m=1}^M S_m$. Remark that the choice of the threshold η depends on the noise level, geometry of $\partial\Omega$ and properties of the inclusion D . Choosing η is thus comparable to choosing a regularization parameter for Tikhonov regularization.

7.2. Reconstruction method B

We call (k, m) a *locally minimal pair* if it satisfies

$$\begin{aligned} I(k, m) &< I(k, m + 1), \\ I(k, m) &< I(k, m - 1), \end{aligned}$$

where $I(k, 0) := I(k, M)$ and $I(k, M + 1) := I(k, 1)$. Corresponding to each locally minimal pair (k, m) we exclude a narrow cone with vertex at y_k , opening direction ω_m , and opening angle $0 < \kappa < \pi/(2n)$. More precisely, we use the following algorithm:

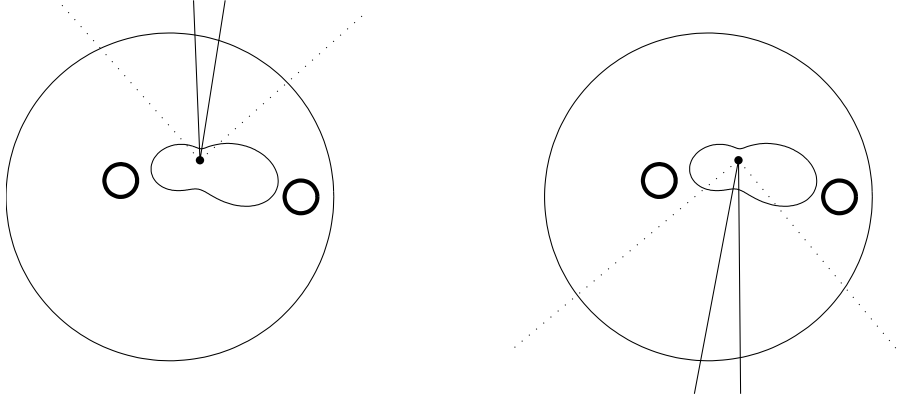


Figure 4. Excluding narrow cones corresponding to locally minimal analyzing cones. Here y is fixed and denoted by a dot. The function $|I_{(y, \cdot)}^{1/n, nN}|$ is plotted with thin line in polar coordinates centered at y . The analyzing cones have opening angle $\pi/4$ and are drawn with dotted lines. The excluded cones have opening angle $\kappa = \pi/32$ and are drawn with solid lines. The two circles drawn with thick line show the boundary of the inclusion D ; the conductivity equals 4 inside D and 1 in the background.

Let (k_ℓ, m_ℓ) , $\ell = 1, \dots, L_{\min}$ be an enumeration of the locally minimal pairs.

- (i) Set $\ell = 1$ and $D_0 = \Omega$.
- (ii) If $\ell > L_{\min}$ then stop, else set $D_\ell = D_{\ell-1} \setminus C_{y_{k_\ell}}(\omega_{m_\ell}, \kappa)$.
- (iii) Set $\ell \leftarrow \ell + 1$ and go to (ii).

We consider $D_{L_{\min}}$ to be an approximation to D . See Figure 4 for an illustration of Step (ii).

We remark that the computation at each point y_k is independent of the computations at other points. Thus the algorithm is readily implementable on a parallel computer.

8. Numerical results

In this section we take Ω to be the unit disc and $n = 2$. This means that we probe the inclusion with straight-angle analyzing cones.

We take $N = 8$ corresponding to the number 32 of electrodes in the ACT3 impedance imaging device of Rensselaer Polytechnic Institute. The set of points $\{y_k\}_{k=1}^K$ is

$$\{(1 + j_1 h, 1 + j_2 h) \in \mathbb{R}^2 : j_1, j_2 \in \mathbb{Z}, h = 2/49\} \cap \Omega,$$

leading to $K = 1696$, and we define the finite collection $\{\omega_m\}_{m=1}^M$ by taking $M = 50$ in (7.1). Discrete ND maps \mathcal{R}_γ^{16} are computed by solving the Neumann problem (6.4) with the finite element method using first-order elements and a triangular mesh with 66049 points. We model measurement noise as

$$\tilde{\mathcal{R}}_\gamma^{16} = \mathcal{R}_\gamma^{16} + [\epsilon_{ij}] + \sqrt{-1} [\epsilon'_{ij}],$$

where the entries of the matrices $[\epsilon_{ij}]$ and $[\epsilon'_{ij}]$ are normally distributed, independent random numbers with one of the following standard deviations:

$$\begin{aligned}\sigma_1 &= 0.0001 \cdot \max_{ij} |\mathcal{R}_\gamma^{16}[i, j]|, \\ \sigma_2 &= 0.001 \cdot \max_{ij} |\mathcal{R}_\gamma^{16}[i, j]|.\end{aligned}$$

The noise level σ_1 corresponds to that of the ACT3 device.

Let us define ρ as the largest real number satisfying

$$\frac{|E_{1/2}(z) - E_{1/2}^{16}(z)|}{\max_{|z| \leq \rho} |E_{1/2}(z)|} \leq 0.03 \quad \text{for all } |z| \leq \rho.$$

By numerical computation we find the approximation $\rho \approx 2$. We interpret this result so that we can safely take $\rho = 1$ in (7.4), leading to

$$\tau_k = \frac{1}{1 + |y_k|}.$$

Note that $\frac{1}{2} \leq \tau_k \leq 1$.

All computations are carried out by Matlab version 6.5 running in a desktop PC computer equipped with a 2.7 GHz Intel Pentium IV processor and 1 GB of RAM. The implementation we use is optimized for clarity, not for speed. In particular, we use nested for-loops in Matlab, which is notoriously inefficient. As a result, the computation of the discrete indicator function takes 2 hours for each example. However, the computation time can be reduced by several orders of magnitude by using another programming language and parallelizing the computation.

8.1. Reconstruction method A

We demonstrate the first numerical algorithm outlined in Section 7.1 by considering one example conductivity with background 1 and two disc inclusions with conductivity 4. We choose $\rho = 0.04$ as threshold. See Figure 5. We reconstruct the convex hull of D but cannot distinguish two inclusions.

8.2. Reconstruction method B

We demonstrate the second numerical algorithm outlined in Section 7.2 by considering two types of example conductivities. We choose $\kappa = \pi/32$ for all examples.

First set of conductivities. We take background conductivity to be 1 and choose at most three disc inclusions with conductivity 4. The radius of the disc inclusions is 0.1. See Figure 6 for plots of indicator functions at fixed points y_k and as function of ω . See Figure 7 for reconstructions of D from noisy and non-noisy data. See Figure 8 for the effect of noise on the indicator function.

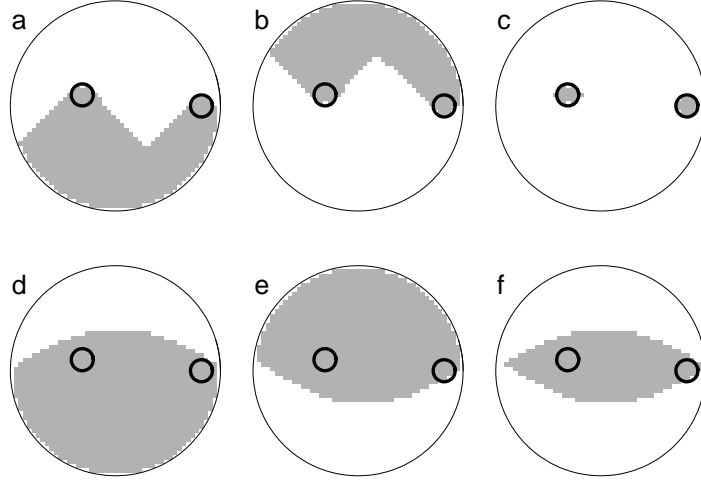


Figure 5. Reconstruction method A. Here Ω is the unit disc and inclusions are the discs drawn with a thick line. (a) Gray color indicates the set of $y \in \Omega$ for which the cone $C_y((0, 1), \pi/4)$ intersects the inclusion. (b) The set of y for which the cone $C_y((0, -1), \pi/4)$ intersects the inclusion. (c) Approximate reconstruction of the inclusion as the intersection of (a) and (b). (d) The set of y for which the indicator function with direction $\omega = (0, 1)$ is smaller than threshold in absolute value. (e) As (d) but $\omega = (0, -1)$. (f) Approximate reconstruction of the inclusion as the intersection of (d) and (e). Note that the reconstruction has only one connected component.

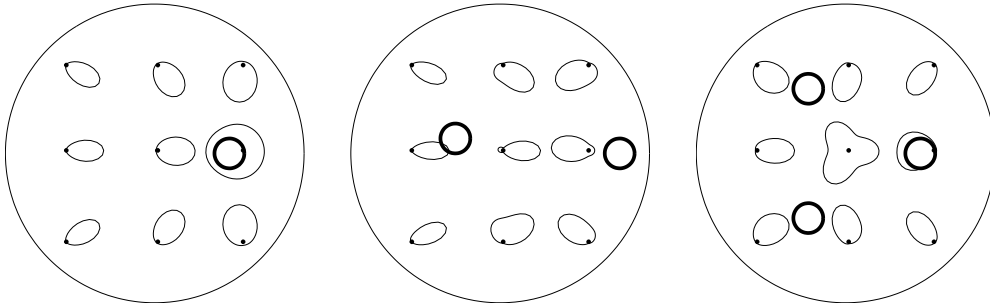


Figure 6. Left to right: Plot of the absolute value of the practical indicator function $I_{(y,\omega)}^{1/2,8}(1/(1+|y|))$ for example conductivities with one, two and three disc inclusions, respectively. The inclusions are plotted with thick line. We plot $|I_{(y,\omega)}^{1/2,8}(1/(1+|y|))|$ with thin line as function of ω at a collection of points y . The plots at various points y are normalized independently of the other points, so quantitative comparison between points is not possible. Inclusions have conductivity 4. The background conductivity is 1.

Second set of conductivities. We take background conductivity to be 1 and introduce a non-convex polygonal kite inclusion. Namely, one of the supposed benefits

of the present reconstruction approach is the possibility to probe inclusions with sharp cones instead of half-spaces, revealing more than the convex hull of D . See Figure 9 for reconstructions.

9. Conclusion

Given a two-dimensional bounded domain and a conductivity distribution, how to extract information about unknown inclusions in conductivity from finitely many noisy Cauchy data? It was proven in [17] that the knowledge of the exact indicator function determines the set of all points in the domain that can be connected with infinity by a straight line without intersecting the closure of the inclusions. In this paper we introduced a truncated indicator function that is computable from a finite number of noisy EIT measurements. Further, we proved that for sufficiently small noise level the truncated indicator function determines the same information than the exact one.

In practical situations the use of the truncated indicator function is limited by significant measurement noise and by the number of electrodes in the EIT system. We gave a parallelizable algorithm for finding approximate information about inclusions in practice. Moreover, we described explicitly how to choose the regularization parameter τ depending on the number of electrodes and the geometry of the domain. We presented a set of numerical examples with computer simulated noisy (continuum model) data. We found that the number and location of inclusions can be reliably estimated. However, the shape of the inclusions was not recovered.

Possible extensions of this approach include three-dimensional version of the algorithm and applications to inverse problems in elasticity or inverse scattering.

Acknowledgements

The authors thank Roland Potthast for valuable discussions. MI was partially supported by Grant-in-Aid for Scientific Research (C)(2) (No. 15540154) of Japan Society for the Promotion of Science. SS was supported by Grant-in-Aid for JSPS Fellows (No. 00002757).

References

- [1] Bateman H 1955 *Higher Transcendental Functions* Vol III, Bateman Manuscript Project (A. Erdélyi, Editor), (McGRAW-HILL, New York)
- [2] Borcea L 2002 Electrical impedance tomography *Inverse Problems* **18** R99–R136
- [3] Borcea L 2003 Addendum to “Electrical impedance tomography” *Inverse Problems* **19** 997–998
- [4] Brown R M and Uhlmann G 1997 Uniqueness in the inverse conductivity problem for nonsmooth conductivities in two dimensions *Commun. Partial Diff. Eqns* **22** 1009–1027
- [5] Brühl M and Hanke M 2000 Numerical implementation of two noniterative methods for locating inclusions by impedance tomography *Inverse Problems* **16** 1029–1042
- [6] Brühl M, Hanke M and Vogelius M S 2003 A direct impedance tomography algorithm for locating small inhomogeneities *Numer. Math.* **93** 635–654
- [7] Calderón A P 1980 On an inverse boundary value problem. *Seminar on Numerical Analysis and its Applications to Continuum Physics* (Society Brasileira de Matemática) pp 65–73
- [8] Cedio-Fengya D J, Moskow S and Vogelius M S 1998 Identification of conductivity imperfections of small diameter by boundary measurements. Continuous dependence and computational reconstruction *Inverse Problems* **14** 553–595
- [9] Cheney M, Isaacson D and Newell J C 1999 Electrical Impedance Tomography *SIAM Review* **41** 85–101

- [10] Dorn O, Miller E L and Rappaport C M 2000 A shape reconstruction method for electromagnetic tomography using adjoint fields and level sets *Inverse Problems* **16** 1118–1156
- [11] Erhard K and Potthast R 2003 The point source method for reconstructing an inclusion from boundary measurements in electrical impedance tomography and acoustic scattering *Inverse Problems* **19** 1139–1157
- [12] Ikehata M 1998 Reconstruction of the shape of the inclusion by boundary measurements *Commun. Partial Diff. Eqns* **23** 1459–1474
- [13] Ikehata M 2002 Reconstruction of inclusion from boundary measurements, *J. Inv. Ill-Posed Problems* **10** 37–65
- [14] Ikehata M 2000 Reconstruction of the support function for inclusion from boundary measurements *J. Inv. Ill-Posed Problems* **8** 367–378
- [15] Ikehata M 2001 The enclosure method and its applications *Analytic Extension Formulas and their Applications* (International Society for Analysis, Applications and Computation, Kluwer Academic Publishers, Dordrecht) **9** pp 87–103
- [16] Ikehata M 2000 On reconstruction in the inverse conductivity problem with one measurement *Inverse Problems* **16** 785–793
- [17] Ikehata M 2004 Mittag-Leffler's function and extracting from Cauchy data *at press*
- [18] Ikehata M 2002 A regularized extraction formula in the enclosure method *Inverse Problems* **18** 435–440
- [19] Ikehata M and Ohe T 2002 A numerical method for finding the convex hull of inclusions using the enclosure method *Electromagnetic Nondestructive Evaluation (VI)* (IOS Press, Amsterdam) pp 21–28
- [20] Ikehata M and Siltanen S 2000 Numerical method for finding the convex hull of an inclusion in conductivity from boundary measurements *Inverse Problems* **16** 1043–1052
- [21] Ito K, Kunisch K and Li Z 2001 Level-set function approach to an inverse interface problem *Inverse Problems* **17** 1225–1242
- [22] Kaipio J P, Kolehmainen V, Somersalo E and Vauhkonen M 2000 Statistical inversion and Monte Carlo sampling methods in electrical impedance tomography *Inverse problems* **16** 1487–1522
- [23] Kirsch A 1998 Characterization of the shape of a scattering obstacle using the spectral data of the far field operator *Inverse Problems* **14** 1489–1512
- [24] Knudsen K 2003 A new direct method for reconstructing isotropic conductivities in the plane *Physiol. Meas.* **24** 391–401
- [25] Knudsen and Tamasan A 2003 Reconstruction of less regular conductivities in the plane, *Aalborg University, Department of Mathematical Sciences Research Reports R-2003-04*, to appear in *Commun. Partial Diff. Eqns*
- [26] Kolehmainen V, Voutilainen A and Kaipio J P 2001 Estimation of non-stationary region boundaries in EIT-state estimation approach *Inverse Problems* **17** 1937–1956
- [27] Mueller J L and Siltanen S 2003 Direct reconstructions of conductivities from boundary measurements *SIAM Journal of Scientific Computation* **24** 1232–1266
- [28] Nachman A 1996 Global uniqueness for a two-dimensional inverse boundary value problem *Ann. of Math.* **143** 71–96
- [29] Novikov R G 1989 Multidimensional inverse spectral problem for the equation $-\Delta\Psi + (v(x) - Eu(x))\Psi = 0$ *Transl. Funct. Anal. and Appl.* **22** 263–272
- [30] Potthast R 2001 *Point sources and multipoles in inverse scattering theory* (Chapman & Hall/CRC Research notes in mathematics **427**)
- [31] Siltanen S, Mueller J L and Isaacson D 2000, An implementation of the reconstruction algorithm of A. Nachman for the 2-D inverse conductivity problem *Inverse Problems* **16** 681–699
- [32] Sylvester J and Uhlmann G 1987 A global uniqueness theorem for an inverse boundary value problem *Ann. of Math.* **125** 153–169
- [33] Uhlmann G 1999 Developments in inverse problems since Calderón's foundational paper *Harmonic analysis and partial differential equations* (The University of Chicago Press, Chicago and London) pp 295–345

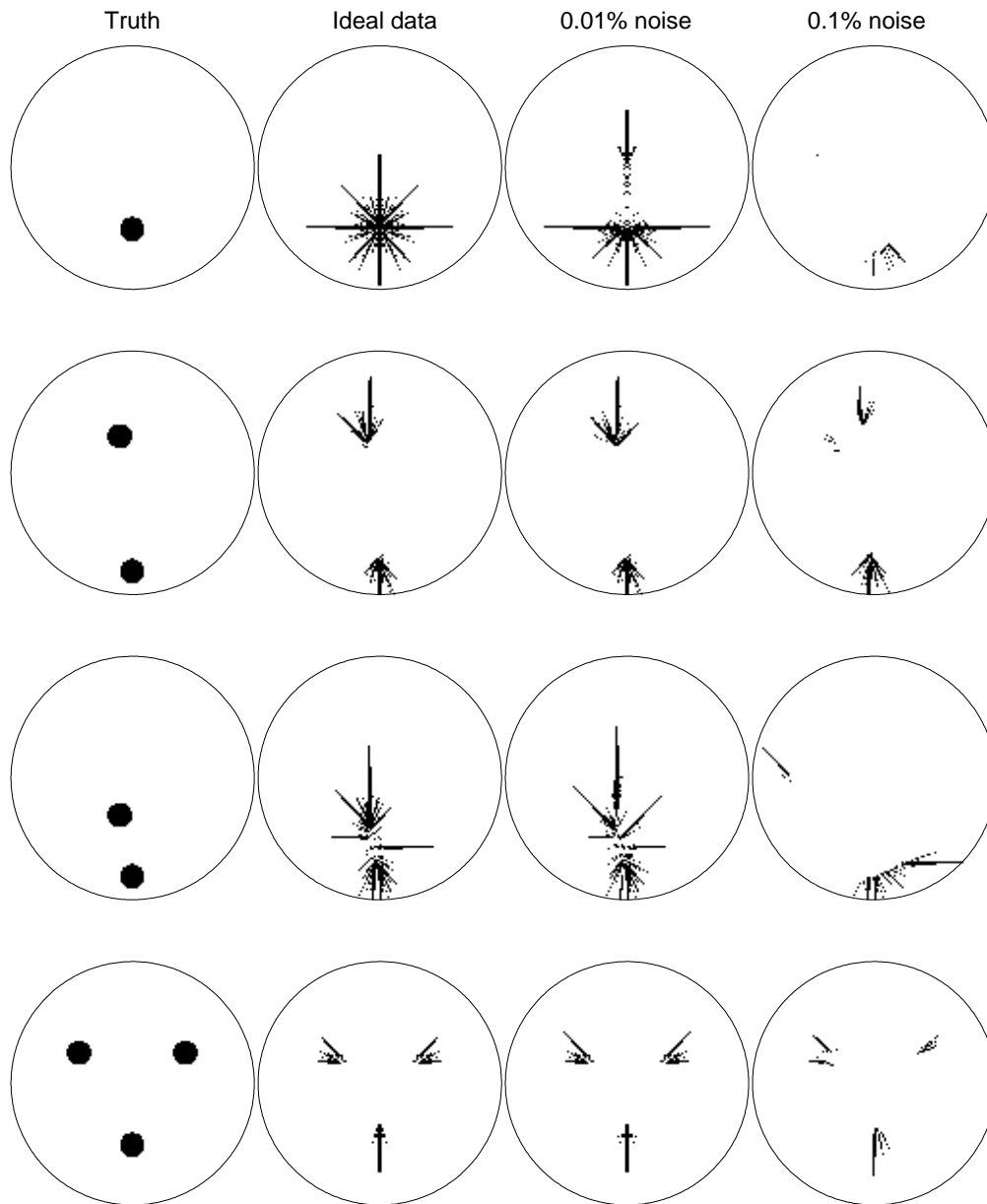


Figure 7. Reconstructions of disc inclusions radius 0.1 and conductivity 4 (first set of examples). Columns from left to right: Original targets with background conductivity 1, reconstructions from ideal data, reconstructions from noisy data with two noise levels.

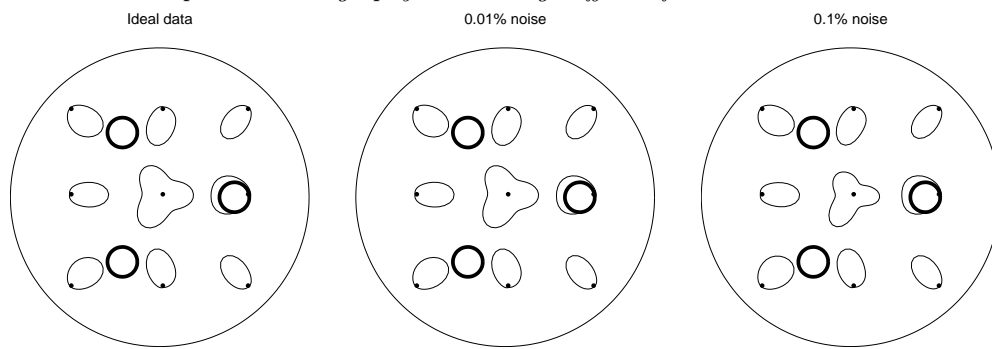


Figure 8. Effect of noise on the indicator function. Compare this figure to the rightmost plot in Figure 6.

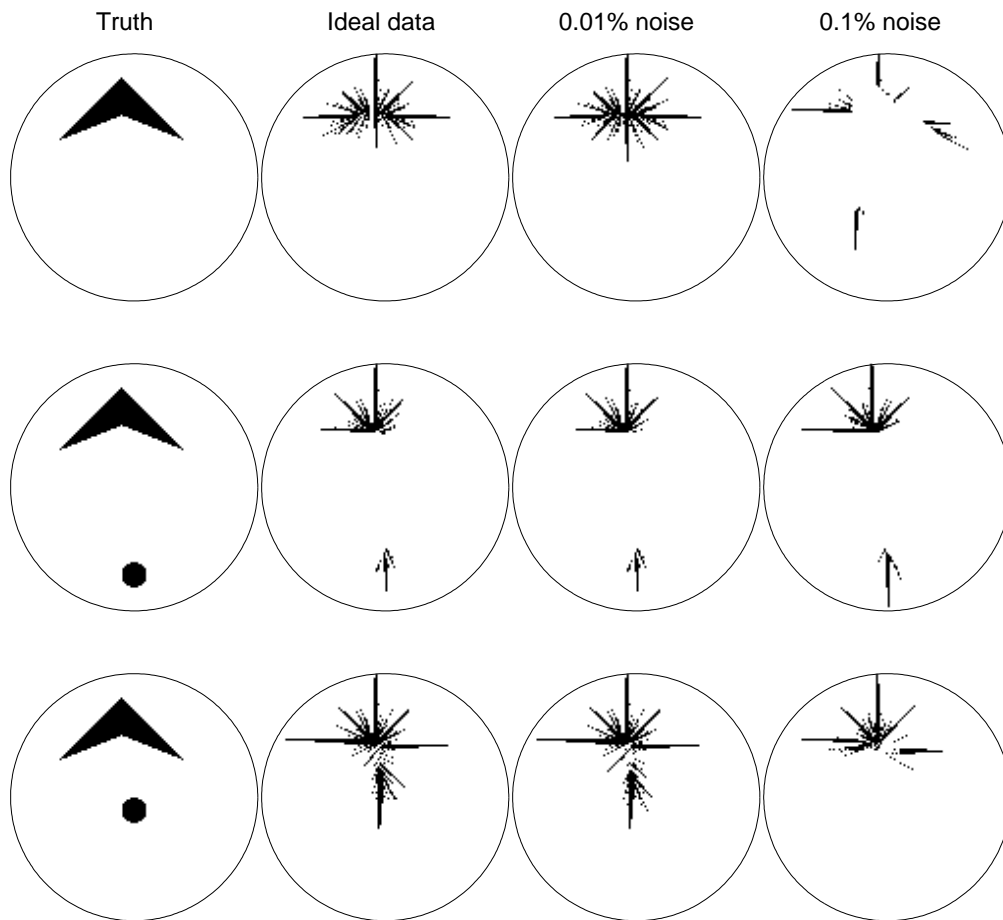


Figure 9. Reconstructions of kite and disc inclusions with conductivity 4 (second set of examples). Columns from left to right: Original targets with background conductivity 1, reconstructions from ideal data, reconstructions from noisy data with two noise levels.